ChemPhotoChem

Chemistry Europe
European Chemical Societies Publishing

# Accepted Article

**Title:** BOPHY Derivatives as Phototherapeutic Agents for the Photodynamic Inactivation of Microorganisms

**Authors:** Claudia Chávez Hernández, Yohana Palacios, Edwin Gonzalez Lopez, Maribel Lopez, Edgardo Durantini, Andres Durantini, Maximiliano Agazzi, and Daniel Alejandro Heredia



**To be cited as:** *ChemPhotoChem* **2024**, e202400077

**Link to VoR:** https://doi.org/10.1002/cptc.202400077

WILEY VCH

10.1002/cptc.202400077

# BOPHY Derivatives as Phototherapeutic Agents for the Photodynamic Inactivation of Microorganisms

Claudia Chávez Hernández,[1†] Yohana B. Palacios,[1†] Edwin J. Gonzalez Lopez,[1] Maribel Lopez,[1] Edgardo N. Durantini,[1,2] Andrés M. Durantini,[3] Maximiliano L. Agazzi,[1*] and Daniel A. Heredia[1,2*]

*1 - Instituto para el Desarrollo Agroindustrial y de la Salud (IDAS), Consejo Nacional de Investigaciones Científicas y Técnicas (CONICET), Ruta Nacional 36 Km 601, X5804BYA, Río Cuarto, Córdoba, Argentina.*

*2 - Departamento de Química, Facultad de Ciencias Exactas, Físico-Químicas y Naturales, Universidad Nacional de Río Cuarto, Ruta Nacional 36 Km 601, X5804BYA, Río Cuarto, Córdoba, Argentina.*

*3 - Department of Chemistry, Southern Illinois University Edwardsville, Edwardsville, Illinois 62026, United States.*

† These authors contributed equally to this work.

[*] Corresponding authors. Tel.: +54 358 4676538; fax: +54 358 76233.
*E-mail address*: magazzi@exa.unrc.edu.ar (M.L. Agazzi).
*E-mail address*: dheredia@exa.unrc.edu.ar (D.A. Heredia).

10.1002/cptc.202400077

**Abstract**

The improvement of photodynamic inactivation (PDI) significantly depends on the development of new families of photosensitizers (PSs). In this sense, three BOPHY derivatives (**BP**, **BP-Br** and **BP-I**) were synthetized, studied, and compared to assess their antimicrobial photodynamic properties. **BP** is an interesting fluorescent probe for cell imaging, while the halogenated analogs (**BP-Br** and **BP-I**) are excellent oxygen photosensitizing agents. **BP** compound presented a fluorescence quantum yield close unity and showed no reactive oxygen species (ROS) production. In contrast, **BP-I** did not show emission properties but exhibited a high production of ROS through both photodynamic mechanisms, generating singlet oxygen (type II) and superoxide radical anion (type I) under aerobic light irradiation. **BP-Br** presented an adequate balance between ROS production and emission properties. The photokilling action and the binding to bacterial cells of these macrocycles were evaluated *in vitro* against methicillin-resistant *Staphylococcus aureus* (MRSA) and *Escherichia coli* bacteria. Our results demonstrated that the halogenated BOPHY derivatives were effective PSs in inactivating MRSA using shorter irradiation periods. In addition, the antimicrobial action sensitized by these BOPHYs was potentiated by adding KI. The combination of halogenated BOPHY and KI led to a complete elimination of both Gram-positive and Gram-negative bacteria. Hence, **BP-Br** and **BP-I** prove to be potent broad-spectrum antimicrobial PSs. To the best of our knowledge, this is the first time that BOPHY derivatives have been applied to photokill pathogenic microorganisms.

**Keywords**: BOPHY, Antimicrobial, Photodynamic Inactivation, Photosensitizer, Bacteria.

## Introduction

The rise in antibiotic resistance represents one of the most severe challenges confronting public health worldwide. The development of new bacterial strains resistant to antibiotics has led to the emergence of complex infectious diseases and the resurgence of previously controlled illnesses.[1,2] Additionally, pharmaceutical companies are increasingly abandoning the antibiotic market due to the less favorable cost-benefit ratio compared to other medications. It takes over 20 years to see any economic benefits from a newly developed antibiotic. During that period, the patent may expire, making it even more challenging to increase profits.[3] Moreover, there is a risk that antibiotic resistance may develop before economic returns are realized, leading to the discontinuation of its commercialization. Thus, the collapse of new antibiotic development in combatting resistant pathogens has led to the exploration of alternative therapies.

In this context, photodynamic inactivation (PDI) has gained attention as a promising antimicrobial therapy for addressing diverse complex infections, including those caused by multiple resistant microorganisms.[4] This alternative approach relies on the combination of three key elements: a photosensitizer (PS), light of an appropriate wavelength, and oxygen. After irradiation of the PS under aerobic conditions, cytotoxic reactive oxygen species (ROS) can be generated by two photodynamic pathways known as type I and type II (Scheme S1).[5] The first pathway is characterized by the generation of free radicals, while the second one involves the production of singlet oxygen ($^1O_2$).[6,7] These ROS have the capability to non-specifically attack various biological substrates, including lipids, proteins, nucleic acids, and others, resulting in the loss of activity in these biomolecules and subsequent cell death.[6,7] Furthermore, the broad spectrum of biomacromolecules affected by ROS leads to multiple and simultaneous cell damages, giving a wide range of inhibitory activity and avoiding the development of resistance by pathogens against PDI.[8,9] The optimization of this therapy crucially hinges on the advancement of novel PSs endowed with appropriate properties. Various families of PSs have been extensively studied in PDI.[5,10,11,12] However, to the best of our knowledge, there is only one report documenting the application of a BOPHY macrocycle in the

photokilling of microorganisms; and in this singular case, the photodynamic activity was attributed to a fullerene $C_{60}$ moiety and not to the BOPHY unit.[13]

The BOPHY core is a dimeric and symmetrical tetracyclic structure consisting of two -$BF_2$ units in six-membered chelate rings, attached to pyrrole units at the periphery. This $BF_2$-based fluorophore, reported for the first time in 2014,[14] exhibits excellent spectroscopic properties, including two absorption bands (between 400 and 500 nm) with high molar extinction coefficients ($\varepsilon > 10^4$ $m^{-1}$ $cm^{-1}$) and high fluorescence quantum yields (close to unity).[15] These spectroscopic properties make this macrocycle an excellent fluorescent probe with potential application for bioimaging.[16,17] However, BOPHY applications are not only limited to their fluorescence properties since the attachment of halogenated atoms to the macrocycle favors the excited triplet state formation by heavy atom effect, with the concomitant capability to produce ROS.[18,19] Thus, we hypothesize that BOPHY cores decorated with halogen atoms can be used as efficient PSs in the inactivation of Gram-positive and Gram-negative bacteria, having an adequate balance between ROS generation and fluorescent properties, turning them into excellent theranostic agents.

Based on these premises, in this investigation, we report the synthesis and characterization of three BOPHY derivatives to study their photodynamic antimicrobial action on pathogenic microorganisms. One dye, **BP-H** (without halogen atoms), is a probe that can be used as a fluorescent imaging agent, and the other two, **BP-I** and **BP-Br** (BOPHY unit with the attachment of halogen atoms), can be used as ROS photosensitizing analogs. Absorption and fluorescence properties of the three macrocycles were studied and compared in diluted acetonitrile (ACN) solutions. Singlet oxygen sensitization mediated by BOPHYs was evaluated using direct and indirect methods. The generation of ROS by type I photodynamic mechanism was assessed by the formation of superoxide anion radical ($O_2^{\bullet-}$), using the nitro blue tetrazolium (NBT) method. The capability of BOPHY to be incorporated by bacterial cells was studied using fluorescence spectroscopy. The antimicrobial action mediated by these PSs was tested *in vitro* against methicillin-resistant *Staphylococcus aureus* (MRSA) and *E. Coli* (*E. coli* EC7, resistant to β-lactam antibiotics). In addition, photokilling of

10.1002/cptc.202400077

microbial cells sensitized by BOPHYs was evaluated in the presence of KI as a potentiation agent. Our results contribute to the development of a new family of BOPHY-based PSs that can be added to the arsenal of existing phototherapeutic agents. Furthermore, this work provides the appropriate conditions for eliminating the Gram-positive and Gram-negative bacteria, highlighting the importance of using KI as an inexpensive approach to increase the antimicrobial action of these $BF_2$-based dyes. As far as we know, this research represents the first application of BOPHY core as broad-spectrum antimicrobial PSs. We pave the way for developing new and more elaborated BOPHY-based PSs to be used in the photoinactivation of pathogenic microorganisms.

## Experimental Section

### *Synthesis of BOPHYs derivatives*

BOPHY macrocycles **BP-H**, **BP-Br** and **BP-I** were prepared following the synthetic sequence shown in **Scheme 1**.

### *2-formyl-3,5-dimethylpyrrole (2)*

Degassed dry *N*,*N*-dimethylformamide (DMF, 975 µL, 12.6 mmol) was cooled in an ice/water bath, and phosphoryl chloride (1.3 mL, 14.2 mmol) was slowly added dropwise under argon atmosphere. The cooling bath was removed, and after reaching room temperature, the solution was stirred for 20 min. Subsequently, the mixture was once again cooled to 0 °C, and a solution of 2,4-dimethylpyrrole (**1**, 1 g, 10.5 mmol) in dichloroethane (DCE, 30 mL) was added dropwise. After removing the ice bath and allowing the reaction to reach room temperature, it was refluxed for 2 hours under an argon atmosphere. Then, upon reaching room temperature, the reaction was poured into cold water adjusted to pH = 12 using NaOH. The mixture was stirred at room temperature for 1.5 h and then extracted twice with dichloromethane (DCM). The organic phase was washed with brine, dried with $MgSO_4$, and evaporated under reduced pressure. The residue was purified by column chromatography (silica gel, hexane/ethyl acetate, 8:2) to give the desired product **2** (1.16 g, 90 %) as a white-yellow solid.[13] $^1$H NMR (500 MHz, $CDCl_3$) δ 9.67 (s, 1H), 9.47 (s, 1H), 5.85 (d, *J* = 2.1 Hz, 1H), 2.32 (s, 3H), 2.30 (s, 3H). The spectroscopic data of **2** were in full agreement with those previously reported in the literature.[20]

### *(1E,2E)-1,2-bis((3,5-dimethyl-1H-pyrrol-2-yl)methylene)hydrazine (3)*

2-formyl-3,5-dimethylpyrrole **2** (1 g, 8.12 mmol) was dissolved in absolute ethanol (EtOH, 30 mL), and hydrazine hydrate 50–60% (406 µL, 4.46 mmol) was added dropwise. Afterward, glacial acetic acid (AcH, 50 µL) was added, and the reaction mixture was stirred at room temperature for 2 h. The suspension was cooled to 5 ºC overnight without stirring. The resulting yellow precipitate was

filtered off and washed with cold water. The resulting solid product was dried at 40 °C in vacuo to yield aldazine **3** (1.63 g, 83 %). This Schiff base was used in the next step of the synthesis sequence without further purification. $^1$H NMR (500 MHz, $CDCl_3$) δ 9.01 (br. s, 2H), 8.35 (s, 2H), 5.80 (s, 2H), 2.26 (s, 6H), 2.17 (s, 6H). The NMR spectroscopic data agree with the previously reported data.[14]

***BOPHY (BP)***

Aldazine **3** (1.3 g, 5.36 mmol) was dissolved in toluene (40 mL), and triethylamine (TEA, 14 mL, 0.1 mol) was added under argon atmosphere. The resulting solution was stirred for 20 min at room temperature, and $BF_3{\cdot}OEt_2$ (19 mL, 0.15 mol) was added. After that, the reaction mixture was refluxed for 18 h, quenched with water, extracted with DCM, and dried over $MgSO_4$. The organic solvent was removed under reduced pressure, and the crude was chromatographed (silica gel, DCM/cyclohexane, 7:3) to afford BOPHY **BP** (925 mg, 74 %). $^1$H NMR (400 MHz, $CDCl_3$) δ 7.94 (s, 2H), 6.18 (s, 2H), 2.49 (s, 6H), 2.33 (s, 6H). The NMR spectroscopic data agree with the previously reported data.[14]

***BOPHY-Br$_2$ (BP-Br)***

**BP** (400 mg, 1.18 mmol) was dissolved in α,α,α-trifluorotoluene (TFT, 7 mL), and *N*-bromosuccinimide (NBS, 630 mg, 2.96 mmol) was added. The resulting solution was stirred at room temperature for 25 min. The consumption of the starting material was monitored by thin-layer chromatography (TLC). After that, DCM was added and the resulting solution was washed with water. The organic solvent was removed under reduced pressure. The crude was purified by column chromatography (silica gel, hexane/DCM, 1:1) to give the brominated BOPHY **BP-Br** (94 %, 557 mg). $^1$H NMR (500 MHz, $CDCl_3$) δ 7.97 (s, 2H), 2.53 (s, 6H), 2.31 (s, 6H).

***BOPHY-I$_2$ (BP-I)***

**BP** (468 mg, 1.38 mmol) was dissolved in chloroform (20 mL), and then a solution of ICl (630 mg, 3.88 mmol) in methanol (MeOH, 10 mL) was slowly added to it. The reaction mixture was stirred at room temperature for 1.5 hours. After a few minutes of starting the reaction, a precipitate (product) was observed. After that, DCM was added, and the resulting solution was washed with a saturated solution of sodium thiosulfate and brine. The organic phase was dried over $MgSO_4$ and evaporated in a vacuum. The crude was chromatographed (silica gel, hexane/DCM, 2:3) to afford the diiodo compound **BP-I** (760 mg, 93 %). $^1$H NMR (400 MHz, $CDCl_3$) δ 8.00 (s, 2H), 2.56 (s, 6H), 2.31 (s, 6H).

***Spectroscopic characterization***

Absorption and emission properties were studied by UV-visible absorption and steady-state fluorescence spectroscopies. Absorption spectra of BOPHYs were acquired in diluted solutions of ACN in a quart cell (1 cm path length). Solutions with absorbance of 0.07 at λ = 450 nm were used to obtain the fluorescence spectra ($\lambda_{exc}$ = 450 nm). The fluorescence quantum yields ($\Phi_F$) of **BP-Br** and **BP-I** were calculated by comparing their emission spectra area with that obtained for the reference (**BP**, $\Phi_F$ = 0.71), according to the previously reported procedure.[13,21] The $\Phi_F$ of **BP** was determined using a similar procedure, with the value of **BP** ($\Phi_F$ = 0.92 in toluene)[14] as the reference and corrected for the refractive index of the solvents (Equation S1). Excitation spectra of BOPHY macrocycles were determined in ACN by monitoring the emission at $\lambda_{em}$ = 530 nm. Spectroscopic experiments were performed at room temperature. The molar absorption coefficients (ε) of each BOPHY in ACN were determined at 25 °C using the Beer-Lambert law. Eight solutions of different concentrations were prepared, and the absorbance at the maximum absorption was recorded. The values of epsilon (ε) were determined from the slope of the plot of A vs. concentration (Figure S1).

***Detection of $O_2^{\bullet-}$ – type I process***

Production of $O_2^{\bullet-}$ was evaluated using the NBT method. BOPHY derivatives were added to a solution of NBT (0.2 mM) and reduced nicotinamide adenine dinucleotide (NADH, 0.5 mM) in DMF / 10% $H_2O$ until the absorbance reached 0.3 at $\lambda$ = 440 nm. These air-equilibrated solutions were irradiated at $\lambda$ = 440 nm (0.45 mW/cm$^2$), and the absorbance corresponding to the formation of diformazan was monitored at $\lambda$ = 560 nm as a function of irradiation time. A BOPHY-free solution with NBT/NADH and a solution with BOPHYs/NBT but without NADH were irradiated as control experiments.[22]

***Detection of $^1O_2$ – type II pathway***

Photogeneration of $^1O_2$ was carried out by both indirect and direct methods. For the first one, 9,10-dimethylantracene (DMA) was used as a scavenger of $^1O_2$. Aerobic solutions of the trapping reagent and the corresponding BOPHY derivative (A = 0.1 at $\lambda$ = 430 nm) in ACN were irradiated with light at $\lambda$ = 430 nm (0.38 mW/cm$^2$). DMA consumption was spectroscopically monitored by following the decrease in its characteristic absorption band at $\lambda$ = 377 nm. With these absorption data, $ln(A_0/A)$ vs. $t$ (irradiation time) was plotted for each PS, where $A_0$ and $A$ represent the absorptions at the initial time and at time $t$ of irradiation, respectively. The observed rate constants ($k_{obs}$) were determined from the slope of the linear fit of these Stern-Volmer plots. The singlet oxygen quantum yield ($\Phi_\Delta$) was determined by comparing the $k_{obs}$ of each BOPHY relative to the reference tetraphenylporphyrin (TPP) ($\Phi_\Delta$ = 0.60[23]).[21,22]

The measurement of $^1O_2$ luminescence at 1270 nm was conducted using the steady-state phosphorescence technique (direct method) with a Horiba/Jobin Yvon Fluoromax-4 spectrofluorometer (HORIBA Scientific). Spectra were obtained during continuous irradiation of BOPHY solutions ($A^{445\ nm}$ = 0.3) in ACN at a wavelength of 445 nm. A 90 º photon emission collection configuration was employed. A cutoff filter with a wavelength cutoff of 1200 nm was placed to eliminate signals at wavelengths shorter than the cutoff, thus favoring the detection of $^1O_2$.

The excitation wavelength was chosen based on the absorption maxima of the PSs under study and the emission spectrum of the excitation lamp.

### *Microorganism and growth conditions*

PDI treatments and incorporation experiments were carried out using both Gram-positive (MRSA) and Gram-negative bacteria (*E. coli* EC7, resistant to β-lactam antibiotics). The culture media and materials employed were sterilized prior to the study. This process was conducted using an autoclave (All America, Model 25x-2, Manitowoc, USA) at 20 psi and temperatures ranging from approximately 115°C to 121°C for 30 minutes. For isolation, both strains were streaked on sterile Petri dishes (10 cm diameter) containing tryptic soy agar (TSA) and incubated at 37°C for 24 hours. A single colony from each culture was inoculated into culture tubes (Pyrex, 13 × 100 mm) containing 4 mL of tryptic soy broth (TSB). Bacteria were grown for 24 h at 37 °C. Subsequently, aliquots of 100 µL were transferred to tubes containing 4 mL of fresh medium (TSB). The strains were cultured on a rotary shaker (100 rpm) at 37°C until the mid-logarithmic growth phase (A ~ 0.6 at λ = 660 nm for MRSA and A ~ 0.4 at λ = 660 for *E. coli*). Bacteria in the log growth phase were isolated from the medium by centrifugation (3000 rpm for 15 min) of the culture broths and resuspended in 4 mL of phosphate buffer saline (PBS, pH=7.4). This procedure allowed obtaining cultures of ~$10^8$ colony forming units (CFU) per milliliter. For both strains, the number of viable cells in CFU/mL was determined on TSA plates after incubation at 37°C for 24 hours (by the spread plate technique using serial dilutions 10-fold in PBS). Samples were streaked on TSA plates in triplicate.

### *PDI treatments*

In all experiments, 2 mL of bacterial suspensions (~$10^8$ CFU/mL) were used, and each BOPHY was added from a stock solution in DMF (1x$10^{-3}$ M). Bacterial suspensions and the corresponding PS (1 and 5 µM for MRSA and *E. coli*, respectively) in PBS were incubated at 37°C for 15 minutes in the dark. Aliquots of bacterial suspensions (200 µL) were transferred to 96-well

plates. The wells were exposed to visible light (350-800 nm, 90 mW/cm$^2$) for different time intervals (5, 15, and 30 minutes). Bacterial suspensions (irradiated, kept in the dark, and controls) were serially diluted with PBS, and each dilution was plated onto TSA plates in sextuplicate, using the micro-drop technique (20 µL). The plates were then incubated at 37°C for 24 hours. Afterward, the number of CFU formed in each micro-drop was counted. The addition of DMF (< 1% V/V) did not exhibit toxicity to microbial cells.

***Binding of BOPHYs to MRSA and E. coli***

Bacteria cells (MRSA and *E. coli*) were cultured in TSB and resuspended in PBS (~1× $10^8$ UFC/mL). Subsequently, 1 mL of the bacterial suspension was added to an Eppendorf tube and treated with the corresponding BOPHY during different incubation times (2, 5, 15, and 30 min) in the dark at 37 °C. BOPHYs stock solutions (1 mM) were prepared in ACN. The concentration of each BOPHY was 1 µM for MRSA and 5 µM for *E. coli*. After the designated incubation time, the cell suspension was centrifugated (14000 rpm, 1 min) in an Eppendorf ultracentrifuge. The supernatant was discarded, and the pellet was resuspended in 1 mL of 2% aqueous sodium dodecyl sulfate (SDS) and incubated overnight at 4 °C in the dark. Afterward, the samples were sonicated for 30 min to complete the cell lysis. Subsequently, 1 mL of SDS solution was added and transferred to a quartz cell to measure the fluorescence emission. The fluorescence intensity of each BOPHY present in the lysate was measured through spectrofluorimetry ($\lambda_{exc}$ = 439 nm, $\lambda_{em}$ = 481 nm for **BP**; $\lambda_{exc}$ = 450 nm, $\lambda_{em}$ = 492 nm for **BP-Br**; and $\lambda_{exc}$ = 456 nm, $\lambda_{em}$ = 496 nm for **BP-I**). The concentration of BOPHY in the lysate was determined by using a calibration curve obtained from measurements of different concentrations of BOPHY in 2% SDS, ranging from 0.25 µM to 3 µM (as shown in Figure S2). The total number of cells was considered to determine the amount of BOPHY bound to the bacteria.[24]

***Potentiation with KI***

PDI treatments in the presence of KI were conducted following a methodology similar to that

described earlier. Bacterial suspensions were treated with 100 mM KI (added from a stock solution in water, 1.0 M). After that, cultures were incubated for 15 minutes in darkness at 37 °C. Subsequently, the suspensions were incubated with the PS, and the experiments were conducted as mentioned earlier in 96-well microtiter plates.

***Formation of iodine***

Air-equilibrated DMF/ water (5 %) solutions containing the corresponding BOPHYs (A = 0.3 at the maximum of the absorption band) and KI (10 mM) were irradiated with white light (350–800 nm, 90 mW/cm$^2$) for 5 min. Absorption spectra were acquired for each solution at room temperature using a quartz cell (10 mm path length). Solutions without KI or BOPHYs were used as negative control experiments, and a Lugol solution was utilized as a positive control. Additionally, solutions containing each BOPHY and KI were bubbled with argon (remotion of oxygen) to demonstrate that ROS generation is essential for forming iodine. The latter was determined by monitoring its characteristic absorption band at $\lambda$ = 360 nm.[22]

10.1002/cptc.202400077





## Results and discussion

### *Synthesis of BOPHY derivatives*

The synthetic sequence for preparing the BOPHY derivatives is shown in **Scheme 1**. We started with a classic Vilsmeier-Haack formylation. 2,4-Dimethylpyrrole (**1**) was treated with $POCl_3$ and DMF in refluxing DCE to give the 2-formyl-3,5-dimethylpyrrole (**2**) in 90 % yield. Then, in a first attempt, formyl pyrrole **2** in EtOH was treated with hydrazine hydrate and drops of acetic acid as a catalyst, following the procedure reported by Tamgho et al.[14] However, the reaction yield of this transformation was improved by around 30 % after leaving the reaction mixture overnight at 5 °C. The precipitated product was washed with cold water to afford aldazine **3** as a yellow powder in 83 % yield. Then, we focused on the next task, working towards the construction of the BOPHY macrocycle. The chelation reaction was carried out in a single step by treatment of **3** with TEA and $BF_3{\cdot}Et_2O$ in refluxing toluene. Under these conditions, previously reported by Li et al.,[25] the BOPHY core **BP** was obtained in 74 % yield.

Having established an optimized synthetic pathway for the **BP** macrocycle, our next step was to attach halogen atoms to the BOPHY unit. This approach is useful to promote inter-system crossing (ISC) by covalently binding heavy atoms to the boron dipyrromethene cores.[5] This strategy increases the transition from the singlet excited state to the long-lived triplet state and, consequently, enhances the ROS generation necessary for the antimicrobial action. Thus, attaching bromine or iodine atoms to both pyrrole moieties is an interesting alternative for transforming the BOPHY fluorophore into a PS.[5]

10.1002/cptc.202400077

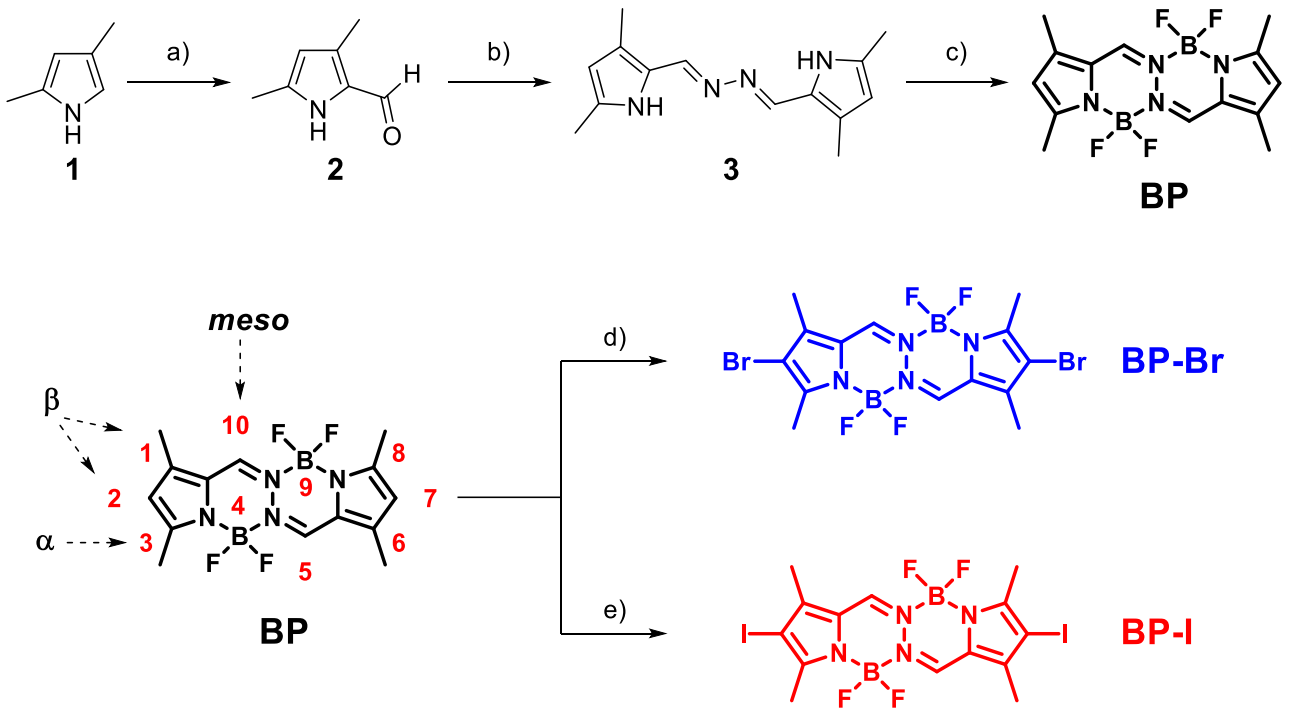


**Scheme 1**. Synthetic route for the obtention of BOPHYs derivatives. Reagents and conditions: a) 1. $POCl_3$, DMF, DCE, 2. NaOH (90 %); b) $NH_2NH_2.H_2O$, AcH, EtOH (83 %); c) TEA, $BF_3{\cdot}Et_2O$, toluene (74 %); d) NBS, TFT (94 %); e) 1. ICl, $CHCl_3$/MeOH, 2. $Na_2S_2O_3$ (93 %).

The first synthesized halogenated compound was the bromide macrocycle **BP-Br**. Among the various protocols that were evaluated, such as NBS/DMF, NBS/$CHCl_3$/AcH and $Br_2$/DCM, the most successful one proved to be the use of NBS and TFT as a solvent. It has been demonstrated that the use of NBS in fluorinated solvents significantly decreases the reaction time for halogenations, resulting in high yields and regioselectivity at positions 2 and 6 of the BODIPY heterocyclic skeleton.[26,27] These reaction conditions, which had previously proved successful for us,[27] allowed the obtention of the halogenated BOPHYs with bromine atoms at positions 2 and 7. The reaction proceeded in short times (25 minutes) with high regioselectivity, yielding 94% after purification through a short pad of silica gel. This finding highlights the potential of NBS and TFT as a powerful new tool for efficient and selective bromination reactions on the BOPHY core.

Based on this previous experience, we attempted to extend the above procedure to prepare the desired 2,7-diiodo derivative (using *N*-iodosuccinimide in TFT). The aromatic electrophilic

substitution under these conditions occurred with high yields but required prolonged reaction times (2 days). Furthermore, it is noteworthy that we achieved control over mono- and di-iodation. On the side, we also explored the classical reaction commonly used for BODIPYs, which involves $I_2$ and $HIO_3$.[5] However, the optimal conditions were those reported by Huaulmé et al.[28] **BP** was treated with iodine monochloride at room temperature, and the reaction progress was monitored by TLC. After 1.5 h, TLC analysis revealed the consumption of starting material and the appearance of a less polar non-fluorescent spot, indicating the formation of the halogenated product. After a conventional work-up using sodium thiosulfate, the crude was subjected to column chromatography over a short pad of silica gel, cleanly affording **BP-I** as an orange solid in 93 % yield.

The molecular structures of **BP**, **BP-I**, and **BP-Br** were confirmed by NMR (Figure S3-S7). As a consequence of the symmetry of the tetracycle, the proton spectrum of all compounds presents few and simple signals. In the aliphatic region, two singlets, each integrating for six protons, can be observed between 2 and 2.75 ppm. These resonances correspond to the four methyl groups around the macrocycle, with the more deshielded signal attributed to the methyl group proximal to the nitrogen. In the aromatic region, around 8 ppm, protons corresponding to positions 10 and 5 give rise to a singlet that integrates for two protons. Regarding the protons at positions 2 and 7, as expected, they are present in **BP** but not in **BP-I** and **BP-Br**. The presence of halogen atoms does not cause any significant shift in the methyl signals near them. Furthermore, the chemical shifts of bromine and iodine compounds are similar.

It is worth highlighting that the synthesis of BOPHYs is generally considered more straightforward than BODIPYs. BOPHYs can be synthesized using relatively simple and well-established synthetic routes, involving easy steps and high yields. This simplicity facilitates their production on a larger scale without encountering significant challenges or complications compared to BODIPY. Additionally, the availability of starting materials for BOPHY synthesis is usually abundant and cost-effective, further contributing to the scalability and production in large quantities.

10.1002/cptc.202400077

As a result, the characteristics of the synthetic sequence of BOPHY ensure an easy future transition of these macrocycles from the laboratory to the marketplace.

### *Spectroscopic properties of BOPHY derivatives*

The spectroscopic properties of all macrocycles were studied and compared in ACN diluted solutions at room temperature. The main absorption and emission features of each compound are presented in **Table 1**. The absorption spectra of **BP**, **BP-Br**, and **BP-I** in ACN are depicted in **Figure 1A**. The three BOPHY macrocycles show their typical electronic transition represented by two main peaks with similar intensity in the visible region between 400 and 500 nm. **BP**, **BP-Br**, and **BP-I** present two absorption peaks at 447/472, 447/445 and 558/558 nm, respectively.[14,15,29] Moreover, as can be observed, the halogen atoms at positions 2 and 7 of the BOPHY core induce small bathochromic shifts due to the resonance donating effect,[18,30] which is more pronounced for I than Br. Moreover, the transition band $S_0 \rightarrow S_2$ at ~350 nm was also observed in the studied solvent. The molar absorption coefficients of the BOPHY macrocycles were determined in the studied solvent and are summarized in **Table 1**.

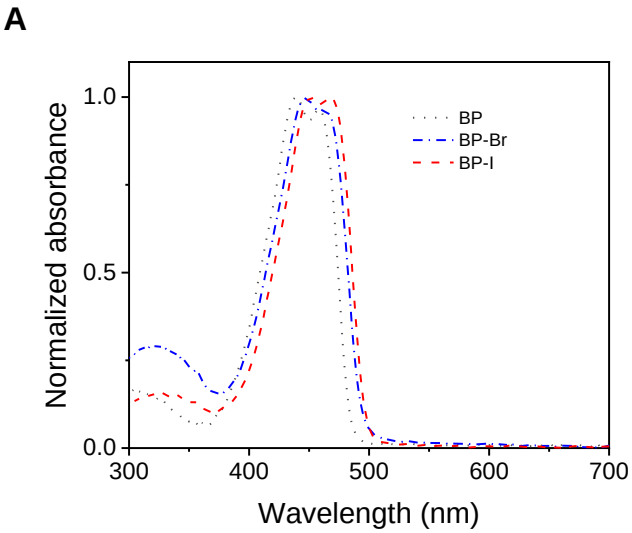

10.1002/cptc.202400077

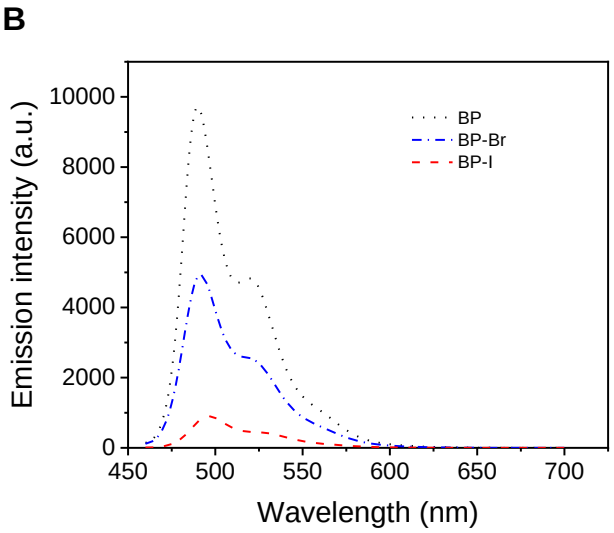


**Figure 1.** (A) Absorption and (B) fluorescence emission spectra ($\lambda_{exc}$ = 450 nm) of **BP** (black dot line), **BP-Br** (blue dash-dot line), and **BP-I** (red dash line) in ACN diluted solution. Fluorescence spectra were acquired from solutions with absorbance of 0.07 at λ = 450 nm. Spectra were acquired at room temperature. [BOPHY] = 1.5 μM.

The fluorescence emission spectra of **BP**, **BP-Br**, and **BP-I** were recorded in ACN (**Figure 1B**), with the samples excited at λ = 450 nm. **BP** displayed highly efficient fluorescence emission, characterized by two prominent bands centered at 482 nm and 510 nm. **BP** exhibited a high fluorescence quantum yield ($\Phi_F$ = 0.71), which agrees with previously reported values.[13,15] The emission spectra of **BP-Br** and **BP-I** exhibited similar characteristics to **BP**, with small bathochromic shifts according to the redshift of their absorption spectra. The emission was significantly quenched for the diiodo derivative, resulting in a $\Phi_F$ value of 0.09. Halogen-substitution favors intersystem crossing to the triplet state by heavy atom effect, resulting in a drop in the fluorescence quantum yield. In the case of **BP-Br**, the minor heavy atom effect results in an appreciable fluorescence yield close to 0.40. This value makes **BP-Br** suitable for fluorescence bioimaging applications and useful as a marker to locate and quantify the compound in the intracellular environment. The $\Phi_F$ values of the BOPHYs are in accordance with those previously reported for similar structures.[18,30] Furthermore, studies have demonstrated that BOPHYs generally exhibit higher fluorescence quantum yields

(regardless of solvent polarity) compared to BODIPY, making them better fluorophores in relation to their BODIPY counterparts.[29,31]

Fluorescence excitation spectra of BOPHY derivatives were recorded in ACN at room temperature while monitoring the emission at $\lambda$ = 530 nm. As can be observed in Figure S8, all macrocycles exhibit similar excitation spectra, showing a profile reminiscent of their UV-visible absorption spectra in ACN. This suggests that individual species emit in the organic solvent, indicating that BOPHY macrocycles are not aggregated in ACN. Fluorescence excitation spectroscopy is a highly sensitive technique capable of distinguishing and examining the UV-visible absorption bands of the phototherapeutic agent, even at very low concentrations. Moreover, the excitation spectrum is particularly valuable for discerning absorption bands when BOPHY is present in biological media, as the absorption spectrum may overlap with other chromophores.[32]

The singlet excited state energy levels for **BP**, **BP-Br**, and **BP-I** were determined by analyzing the intersection points of absorption and fluorescence bands, as outlined in **Table 1**. Stokes shifts, calculated from the maxima of the absorption and fluorescence spectra, exhibited values of 24, 29, and 28 nm for **BP**, **BP-Br**, and **BP-I**, respectively. These moderate Stokes shifts of around 30 nm indicate a structural alteration between their excited ($S_1$) and ground states ($S_0$), underscoring the molecular lower rigidity of these compounds compared to other pyrrolic macrocycles. For example, BOPHYs have higher Stokes shifts than BODIPY, a closely related macrocycle with a similar molecular structure (although the substitution pattern must be taken into consideration).[28,31] This behavior resulting from the different geometries of the excited and ground states, combined with the appropriate emission, renders them excellent candidates as organic fluorophores for use in fluorescence bioimaging. Large Stokes shifts reduce self-absorption and self-luminescence, thereby enhancing detection accuracy and resolution in fluorescence imaging.[33]

**Table 1.** Spectroscopic and photodynamic properties of **BP, BP-Br** and **BP-I** in ACN.

| Compound | $\lambda_{max}^{abs}$ (nm) | $\varepsilon$ ($M^{-1}cm^{-1}$) | $\lambda_{max}^{em}$ (nm)[a] | Es (eV) | $\Phi_F$[b] | $k_{obs}$ / 1 × $10^{-4}$ ($s^{-1}$)[c] | $\Phi_\Delta$[d] |
|---|---|---|---|---|---|---|---|
| **BP** | 439, 458 | 44400 | 482, 510 | 2.64 | 0.71 | 0.70 ± 0.02 | 0.17 |
| **BP-Br** | 447, 463 | 47600 | 492, 520 | 2.60 | 0.39 | 1.50 ± 0.04 | 0.37 |
| **BP-I** | 451, 468 | 44060 | 496, 528 | 2.57 | 0.09 | 2.67 ± 0.01 | 0.66 |

[a] $\lambda_{exc}$ = 450 nm. [b] Reference **BP** in toluene: $\Phi_F = 0.92$.[13] [c] Fitting error reported. [d] Reference TPP in ACN: $k_{obs} = 2{,}43 \times 10^{-4}\ s^{-1}$, $\Phi_\Delta = 0.6$.[23]

### *$^1O_2$ photosensitization*

As previously mentioned, there are two mechanisms by which ROS can be generated. One of them, known as type II, involves the absorption of light by the PS to reach its excited triplet state ($^3PS^*$), followed by an energy transfer process to molecular oxygen ($^3O_2$), resulting in the formation of $^1O_2$.[34] This cytotoxic ROS plays a crucial role in the PDI treatments since its powerful oxidizing capacity and elevated reactivity allow it to react and damage a wide range of biomacromolecules non-specifically.[35] Thus, this ROS is a valued bactericidal species that must be evaluated to determine the potential of a compound to be used as a PS. To that end, the photosensitizing capacity of BOPHYs to generate $^1O_2$ was assessed through direct and indirect methods.

The evaluation through the indirect method was carried out through the photodecomposition of DMA (9,10-dimethylantracene) in air-equilibrated ACN solutions. DMA is a trapping reagent that chemically and rapidly reacts with $^1O_2$ to produce the 9,10-endoperoxide compound (Scheme S2). Thus, the photooxidation reaction of the scavenger was followed by UV-visible spectroscopy, monitoring the consumption of DMA through the decrease of its characteristic absorption band at $\lambda^{DMA}$ = 377 nm. Chemical trap decomposition sensitized by all BOPHYs was performed upon irradiation at $\lambda_{irr}$ = 430 nm.

Absorption spectra of the DMA in the function of the irradiation time are shown in Figure S9. As can be observed, there is a gradual decrease in DMA absorption bands as the irradiation time increases, which means that $^1O_2$ is photogenerated by BOPHYs. However, the consumption of the

quencher at equal intervals of time is not the same for all macrocycles. Furthermore, the distinctive absorption bands of BOPHYs remained constant throughout the measurements, confirming their photostability and retention of their spectroscopic properties under these conditions. This was an expected result since several investigations have proved that BOPHYs have good photostability, even higher than the well-documented BODIPY.[31,36] As control experiments, solutions of each BOPHY and DMA were kept in the dark. After 30 min, no changes were observed in the DMA absorption spectra. In addition, no spectral changes were observed after irradiating ($\lambda_{irr}$ = 430 nm) a DMA solution (Figure S9).

The reaction of $^1O_2$ with DMA induced by the photosensitizing action of BOPHYs follows a pseudo-first-order kinetic behavior, as described by Equation S2. **Figure 2** shows the semilogarithmic plots corresponding to the spectroscopy decay of DMA. As can be seen, the photosensitization of $^1O_2$ exhibits different rates, with the halogenated compound being the most efficient in producing ROS. This can be demonstrated and quantified by the different $k_{obs}$ values (**Table 1**). The $k_{obs}$ values for **BP**, **BP-Br**, and **BP-I** were determined from the slope of each linear fit. Subsequently, these values were compared with that for the reference (tetraphenylporphyrin, TPP) to determine the $\Phi_\Delta$ of BOPHY derivatives, which are also recorded in **Table 1**. $\Phi_\Delta$ values were 0.17, 0.37, and 0.66 for **BP**, **BP-Br**, and **BP-I**, respectively. **BP** has the lowest $\Phi_\Delta$ value, indicating that its $^1O_2$ production is insignificant. This result was expected, considering the high $\Phi_F$ of **BP**. The highest $\Phi_\Delta$ was that obtained for the diiodo derivative ($\Phi_\Delta$ = 0.66). This value closely resembles that obtained from a BOPHY-$C_{60}$ dyad.[13] In that system, BOPHY served as a visible light-harvesting antenna, while the fullerene $C_{60}$, known for being one of the most efficient PS in producing ROS, carried out the photodynamic action. The $\Phi_\Delta$ for the BOPHY-$C_{60}$ dyad, obtained under similar conditions, was 0.76. Consequently, BP-I exhibits an outstanding capacity to generate $^1O_2$, with a quantum yield comparable to that of fullerene derivatives. Even **BP-I** presents higher values than several $C_{60}$ cycloadducts.[10] In relation to **BP-Br**, $\Phi_\Delta$ value is suitable for application in photodynamic treatments,

being similar to certain BODIPY.[5] Finally, these results confirm that **BP-Br** and **BP-I** undergo a type II photoprocess after light irradiation.

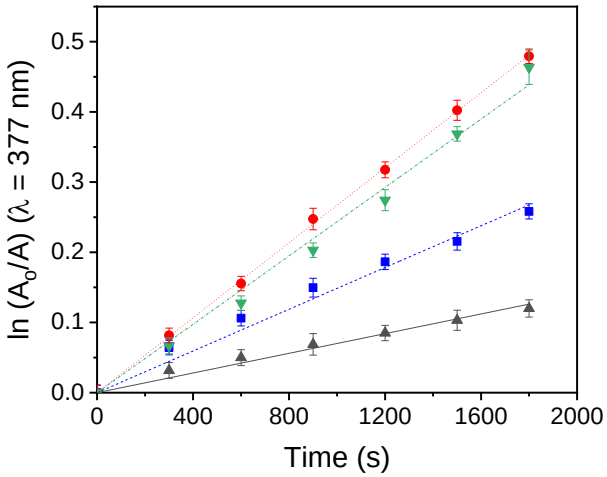


**Figure 2**. First-order plots for the consumption of DMA photosensitized by BOPHYs. **BP** (black up-pointing triangle), **BP-Br** (blue square), **BP-I** (red circle), and TPP (green down-pointing triangle) in air-equilibrated ACN solution ($\lambda_{irr}$ = 430 nm, 0.38 mW/cm$^2$). Values represent the mean ± standard deviation of three consecutive experiments. $A_{PS}$ = 0.1 at 430 nm, [PS] ~ 2.2 µM.

To further strengthen and provide additional evidence of the formation of $^1O_2$ sensitized by the BOPHY molecules, steady-state phosphorescence measurements were carried out in ACN under aerobiosis, monitoring the emission around 1270 nm attributed to $^1O_2$ phosphorescence. Solutions containing the respective BOPHYs exhibit a similar trend to that observed in the indirect method. Specifically, the diiodo BOPHY displays a higher $^1O_2$ production compared to the dibromo macrocycle (Figure S10), reinforcing and furnishing additional data on the generation of this ROS. Taking into account that **BP-I** has a $\Phi_\Delta$ of 0.66 (determined by the indirect method), by comparison of the areas, it is possible to estimate a $\Phi_\Delta$ of around 0.37 and 0.19 for **BP-Br** and **BP-H**. These outcomes are similar to those obtained by the indirect method.

***$O_2^{\bullet-}$ photoproduction***

While the ability to generate $^1O_2$ is an important parameter in a PS, this is not the only reactive species that can be produced after irradiation with visible light in aerobic conditions. Other ROS can be generated through a type I photoprocess. Here, the $^3PS^*$, attained after light absorption, can transfer electrons to biological substrates, resulting in the generation of free radicals, which, in the presence of molecular oxygen, led to the formation of $O_2^{\bullet-}$. This ROS, generated by an electron transfer process, plays a significant role in PDI treatments, and its formation is favored by polar environments and the presence of reducing agents.[34,37]

Within this framework, we assessed the photosensitizing capability of BOPHY compounds to generate $O_2^{\bullet-}$. The nitro blue tetrazolium (NBT) method was utilized to monitor the production of this cytotoxic species generated through a type I mechanism. This method relies on the reduction of NBT through reaction with $O_2^{\bullet-}$, leading to the formation of diformazan, which can be followed spectroscopically (Scheme S3). The reduction of the molecular probe is favored by polar solvents and the presence of NADH (biological reducing agent).[13,21]

Air-equilibrated DMF/$H_2O$ (9.9:0.1) solutions containing the respective BOPHY derivative, NBT, and NADH, were irradiated at $\lambda$ = 440 nm. The formation of diformazan was determined and followed through the increase in its absorption band at $\lambda$ = 560 nm (Figure S11). **Figure 3** depicts the variation in absorption intensity at $\lambda$ = 560 nm as a function of the irradiation time. As can be observed, there is a gradual increase in the diformazan absorption for halogenated BOPHY compounds. Furthermore, these absorbance values are substantially higher than those of the control solution containing only NBT + NADH. The photoreduction of the scavenger was not observed for solutions kept in the dark. These outcomes indicated that halogenated BOPHYs are able to induce the production of $O_2^{\bullet-}$ upon aerobic light irradiation. In the literature, we do not find evidence of experiments that demonstrate the formation of this reactive species using BOPHYs as photosensitizing agents. Therefore, this is the first result showing the capacity of these compounds to generate this type of cytotoxic species. $O_2^{\bullet-}$ is of considerable significance in PDI since, within the cellular environment, it can undergo a dismutation process to generate $H_2O_2$, which is converted into

the highly harmful and reactive oxidant hydroxyl radical (OH•), a process known as the Fenton reaction.[38]

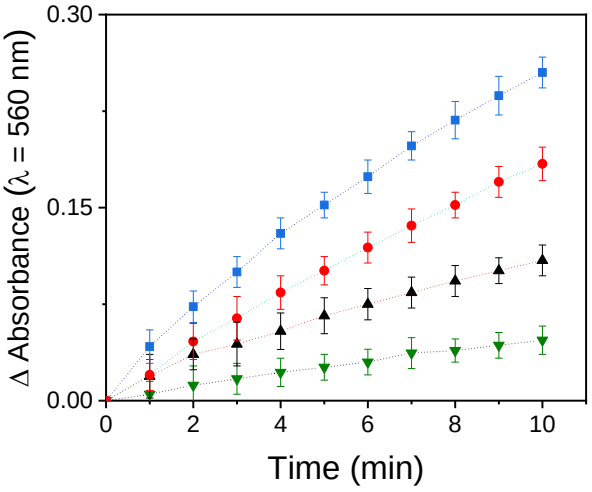


**Figure 3**. Determination of $O_2^{\bullet-}$ production by the NBT method monitoring the characteristic absorption band of diformazan at λ = 560 nm at different irradiation times. Solutions: NBT + NADH (green down-pointing triangle), NBT + NADH + **BP** (black up-pointing triangle), NBT + NADH + **BP-Br** (blue square), NBT + NADH + **BP-I** (red circle) in DMF/$H_2O$ (9.9:0.1). Samples contain NBT (0.2 mM), NADH (0.5 mM) and BOPHYs ($A_{PS}$ = 0.3 at 440 nm, [PS] ~ 6.5 μM). $\lambda_{irr}$= 440 nm (0.45 mW/cm$^2$). Values represent the mean ± standard deviation of three consecutive experiments.

Our photodynamic studies disclosed that the halogenated BOPHY-based PS can produce ROS through type I and type II pathways. Nevertheless, it is crucial to note that the findings observed in solution may not be directly applicable to the cellular environment. Various factors, including the localization and interaction of the PSs with the microenvironment, can significantly influence the photodynamic properties of these compounds.

***PDI treatments***

After verifying the great efficiency in ROS production, we assessed the capability of BOPHYs to act as phototherapeutic agents in the inactivation of bacteria. The photosensitizing activity of **BP**,

**BP-Br**, and **BP-I** was evaluated *in vitro* against a Gram-positive bacterium (MRSA) and a Gram-negative bacterium (*E. coli*). MRSA is a significant contributor to healthcare-associated infections and is endemic in numerous hospitals worldwide.[39] Moreover, this microorganism has developed multi-resistance to clinical antibiotics, limiting therapeutic options for treatment. On the other side, *E. coli* is nearly ubiquitous in the human gastrointestinal tract and is a common cause of diarrheal diseases globally.[40] Additionally, it can lead to urinary tract infections, neonatal bacteremia, and meningitis. The escalating resistance of *E. coli* to antibiotics has resulted in heightened morbidity, mortality, and substantial healthcare costs.

Bacteria cell suspensions of MRSA in PBS (~$10^8$ CFU/mL) were incubated with the corresponding BOPHY compound (1 μM) in the dark at 37 °C for 15 min. Then, the samples were irradiated with white light for 5, 15 and 30 min (fluence rate = 90 mW/cm$^2$) that correspond to light dosages (fluence) of 27, 81 and 162 J/cm$^2$. The viability of cells after the PDI treatments is shown in **Figure 4A**. The survival of microorganisms was not affected by irradiation without BOPHYs and when cells were treated with the BOPHY in the dark. **BP** showed no photoinactivation after 30 minutes of irradiation (162 J/cm$^2$), which is consistent with its photodynamic properties. **BP-Br** and **BP-I** produced a reduction >3.5 log in the cell survival of *S. aureus* using a light dose of 27 J/cm$^2$ (5 min of irradiation). **BP-I** showed a slightly higher inactivation efficiency (4.05 log and 99.991 %) than **BP-Br** (3.83 log and 99.985 %), which is in agreement with its higher $^1O_2$ production yield. Both PSs reach their maximum inactivation after 15 minutes of irradiation (81 J/cm$^2$), resulting in cell viability decreases of 3.95 log (99.989%) and 4.43 logs (99.996%) for **BP-Br** and **BP-I**, respectively.

In *E. coli* cultures (**Figure 4B**), both halogenated BOPHYs showed poor photoinactivation efficiency even at a concentration of 5 mM. After 30 min irradiation, a light dose of 162 J/cm$^2$, these compounds produced a reduction <1 log in the cell survival. The difference in susceptibility may be attributed to the distinct permeability barriers between Gram-positive and Gram-negative bacteria. It is widely recognized that the envelope of *S. aureus* bacteria is less complex and relatively porous, making it more susceptible to a diverse range of PSs, including neutral, cationic, and anionic ones.

Gram-negative bacteria, such as *E. coli*, are known to have a more complex and compact external structure. The highly complex multilayered cell wall, with porin function proteins, is prone to cationic PSs owing to its negatively charged outer envelope.[5] For this reason, *E. coli* is less prone to the action of neutral PSs, and more susceptible to cationic PSs.

Taken together, the results of antimicrobial activity indicate that halogenated BOPHYs present attractive properties to serve as PSs in the PDI of *S. aureus*. In this sense, these compounds can be considered bactericidal or antimicrobial agents according to the American Society of Microbiology since they showed a reduction greater than 3 log CFU (photoinactivation >99.9%).[41] The comparison of the antimicrobial activity of BOPHYs with other PSs is difficult due to the different experimental conditions, including bacterial strains and density, wavelength irradiation, light dosage, treatment protocol, nature and concentration of the PS, among others. Considering this, BOPHYs show interesting properties as alternative PSs to their BODIPY counterparts. For instance, two mono-cationic BODIPYs showed photodynamic efficiencies comparable to the uncharged BOPHYs on *S. aureus*.[42] When cell suspensions were treated with 1 μM BODIPYs, an approximately 4.5 log decrease in viability cell was observed after 5 minutes under visible-light irradiation (21 J/cm$^2$). A brominated bis-cationic $BF_2$-chelated tetraarylazadipyrromethene (4.3 μM, 16 J/cm$^2$, $10^8$ CFU/mL) exhibited a 6.8 and 3.4 log reduction of *S. aureus* and MRSA, respectively.[43] A zinc(II)-dipicolylamine-conjugated dibrominated BODIPY showed a PDI of 4.5 log in *S. aureus* at a concentration of 10 μM and an irradiation dose with green light of 180 J/cm$^2$.[44]

10.1002/cptc.202400077

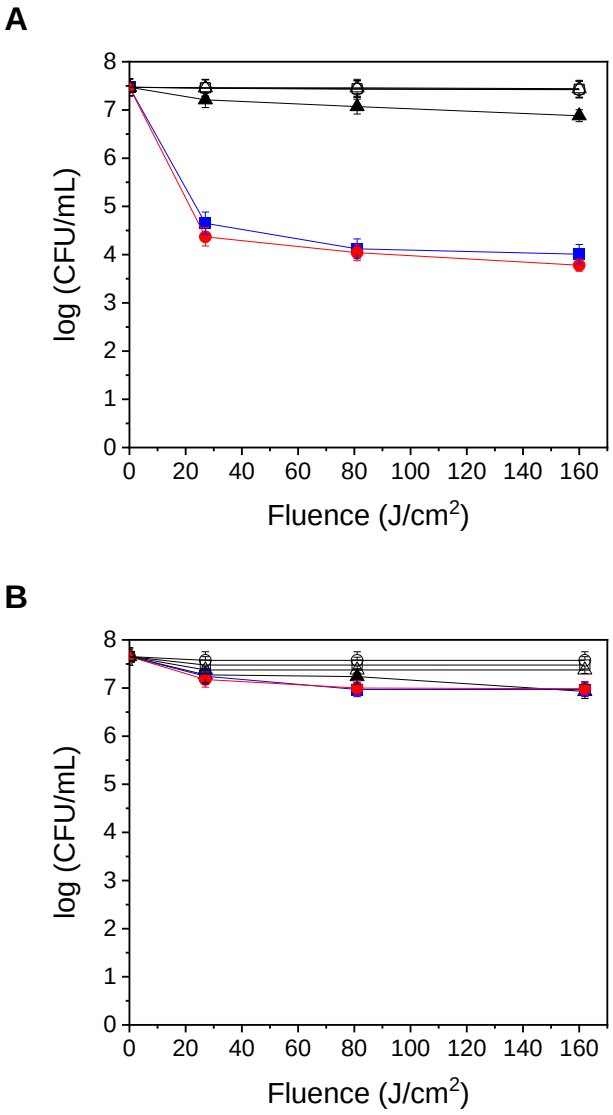


**Figure 4.** Survival curves of (A) MRSA (~$10^8$ CFU/mL) and (B) *E. coli* (~$10^8$ CFU/mL) incubated with each PS and irradiated for different periods (5, 15 and 30 min) with visible light (350-800 nm, 90 mW/cm$^2$): **BP** (black up-pointing triangle), **BP-Br** (blue square), and **BP-I** (red circle). Controls: bacterial cells incubated with **BP** (up-pointing triangle), **BP-Br** (square), and **BP-I** (circle) and non-irradiated. The PS concentrations were 1 μM for MRSA and 5 μM for *E. coli*.

### *Uptake of BOPHYs by bacteria*

Given the disparity observed in the photokilling of microbial cells, particularly the lack of inactivation in Gram-negative bacteria, we sought to assess the capability of BOPHY macrocycles to be incorporated by both pathogenic strains. Bacterial suspensions of MRSA and *E. coli* were treated with 1 μM and 5 μM concentrations of each BOPHY, respectively, maintaining the same

concentration as in the PDI treatments. The uptake of BOPHYs by both bacterial strains after different incubation times can be observed in **Figure 5**. For MRSA, the binding is around 60 %, and it is quickly reached after 2 min of incubation for all BOPHY macrocycles. The quantity of BOPHY bound to the bacterial cells remained relatively constant even after extended incubation periods (30 minutes). When MRSA bacteria were incubated with 1.0 μM of each BOPHY, a mean value of 0.6 nmol/5 × $10^7$ cells was obtained for all of them (**Figure 5A**). A theoretical incorporation of 100% would have been a value of 1 nmol/5 × $10^7$ cells (1 μM in the 2 mL). For *E. coli*, the highest recovered amount of BOPHY was around ~0.55 nmol/5 × $10^7$ cells (**Figure 5B**). These binding values of BOPHYs were reached after 5 min of incubation and represented an average incorporation of ~10 % (5 nmol is the maximum theoretical amount of BOPHYs that can be incorporated).

As mentioned above, the difference observed in the binding of these neutral PS can be attributed to the differences in the cell wall structures of Gram-positive and Gram-negative bacteria.[5] *S. aureus* has a less complex and porous cell wall compared to *E. coli*. The cell wall of *S. aureus* allows various PS, including neutral PS, to permeate easily, facilitating their entry into the bacterial cell.[5,10,45] Conversely, *E. coli*, have a more complex cell wall with an additional outer membrane that acts as a barrier. This outer membrane exhibits lower permeability to neutral molecules, making it challenging for neutral PS to penetrate.[46,47] Cationic PS, which carry a positive charge, are generally more effective against Gram-negative bacteria due to their electrostatic interaction with the negatively charged outer membrane.[5,10]

10.1002/cptc.202400077

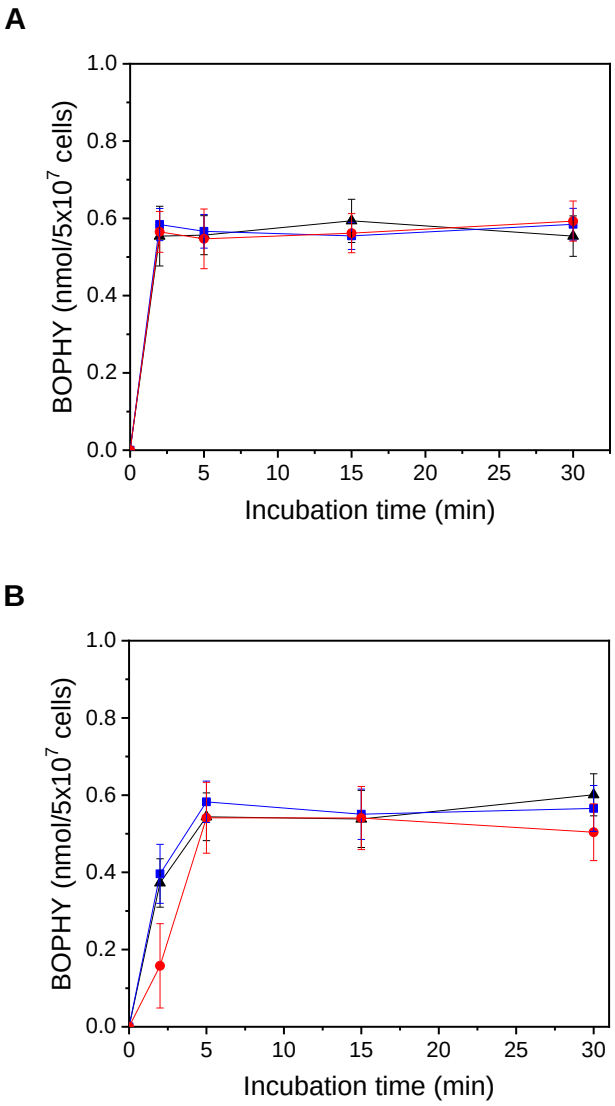


**Figure 5.** Amount of BOPHY recovered for different incubation times at 37 °C in the dark from: (A) MRSA ($5 \times 10^7$ CFU/mL) treated with 1.0 μM **BP** (black up-pointing triangle), 1.0 μM **BP-Br** (blue square), and 1.0 μM **BP-I** (red circle). (B) *E. coli* ($5 \times 10^7$ CFU/mL) treated with 5.0 μM **BP** (black up-pointing triangle), 5.0 μM **BP-Br** (blue square), and 5.0 μM **BP-I** (red circle).

### *Potentiation of PDI with KI*

The enhancement of photodynamic efficacy has been clearly evidenced through the combination of inorganic salts with PS.[48] Potassium iodide has demonstrated remarkable abilities to enhance PDI action.[49] Importantly, KI holds the status of a clinically approved drug with applications in various therapeutic realms, including antifungal treatments.[50]

Thus, with the aim of increasing the photodynamic efficiency, mainly against *E. coli*, we evaluated the PDI of BOPHYs in the presence of KI. **Figure 6** illustrates the survival of both bacteria in cell suspensions (~$10^8$ CFU/mL) containing the corresponding PS and KI. The microbial cells were subjected to a 15-minute treatment with 100 mM KI in the dark at 37 °C, followed by exposure to the PS (1 μM for MRSA and 5 μM for *E. coli*). No toxicity was observed in irradiated cells for 30 minutes with white light in the presence of KI but in the absence of PSs. Additionally, the combination of 100 mM KI and 1 μM PS exhibited no toxicity for microbial cells in the dark. Interestingly, as can be observed in **Figure 6**, the addition of KI noticeably increases the photodynamic efficiency for both halogenated BOPHYs. In MRSA (**Figure 6A**), the potentiation resulted in a reduction in cell survival of approximately >4.5 log (>99.995 % photokilling) for both PSs (**BP-Br** and **BP-I**) after 5 minutes of irradiation (a light dose of 27 J/cm$^2$). This implies an enhancement close to 1 log with respect to the PDI without the potentiating agent. Remarkably, this enhancement was more pronounced during prolonged irradiation times. For example, after 30 minutes of irradiation, a cellular decrease greater than 6 log (>99.9999 % photokilling) was observed for both **BP-Br** (6.26 log) and **BP-I** (6.39 log), indicating an increase of approximately 2 log.

For *E. coli*, the efficiency of the photoinduced treatment was noticeably enhanced with the addition of KI (**Figure 6B**). After 5 minutes of irradiation, an around 3-log reduction in cell survival was observed (2.75 log for **BP-Br** and 3.1 log for **BP-I**), whereas only a <1 log reduction had been previously shown in the salt-free treatment. After a light dose of 162 J/cm$^2$ (30 min of irradiation), the cellular decrease was 3.46 log for **BP-Br** (99.965 %) and 3.96 log for **BP-I** (99.979 %). These findings suggest that, despite their neutral nature, both halogenated PSs have the capability to photoinactivate Gram-negative bacteria when used in conjunction with KI. It is important to mention that, although the incorporation of BOPHYs into *E. coli* is not high, the increase in the inactivation after potentiation could be explained by the reactive iodine species (RIS) generated outside the bacterial cells, which are capable of attacking them.

Similar effects of PDI potentiation mediated by KI were previously observed with various PSs, including tetrapyrrolic macrocycles, BODIPYs, fullerenes, and diketopyrrolopyrroles.[22,51-54] However, there are limited reports of potentiation with KI for neutral PSs against bacteria. Recently, Dabrowski and colleagues observed potentiation of PDI with uncharged porphyrin derivatives (20 μM) in the presence of 100 mM KI.[55] They reported an improvement of 2–3 logs for *S. aureus* and 5 logs for *E. coli* with a low blue-light dose up to 10 J/cm$^2$. Additionally, Calmeiro *et al.* reported similar photoinactivation results for *E. coli* when neutral porphyrins were combined with 100 mM KI. Neutral PSs at concentrations of 1 μM and 5 μM did not result in significant reductions in *E. coli* viability. However, in the presence of salt, a bacterial reduction greater than 4.3 logs was observed after 5 minutes of white light irradiation (7.5 J/cm$^2$).[56]

An important aspect of our study lies in its pioneering exploration of potentiation through the combination of BOPHYs and KI. Our outcomes demonstrate, for the first time, that this combination can be used as a versatile and broad-spectrum treatment, suggesting promising implications for future research. *In vitro* studies demonstrate that BOPHYs can serve as a new family of PSs, which is crucial for expanding the existing arsenal of PSs. This diversification of options plays a pivotal role in addressing the evolving landscape of infectious agents and advancing the field of PDI. By broadening the range of PSs, researchers not only enhance the therapy's versatility but also ensure they have a comprehensive toolkit to combat a wide spectrum of diseases.

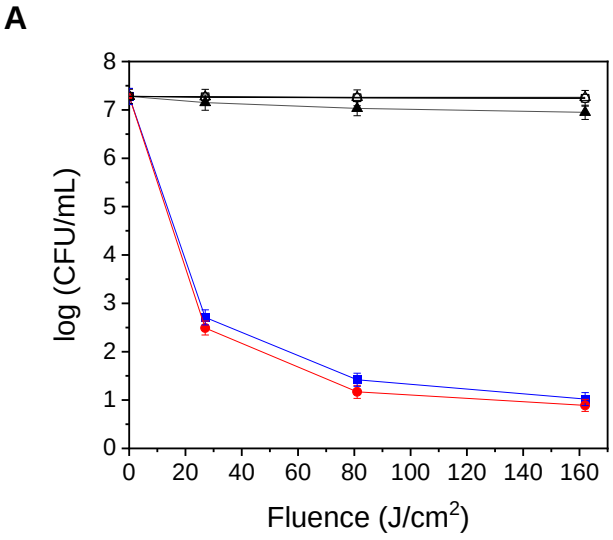

10.1002/cptc.202400077

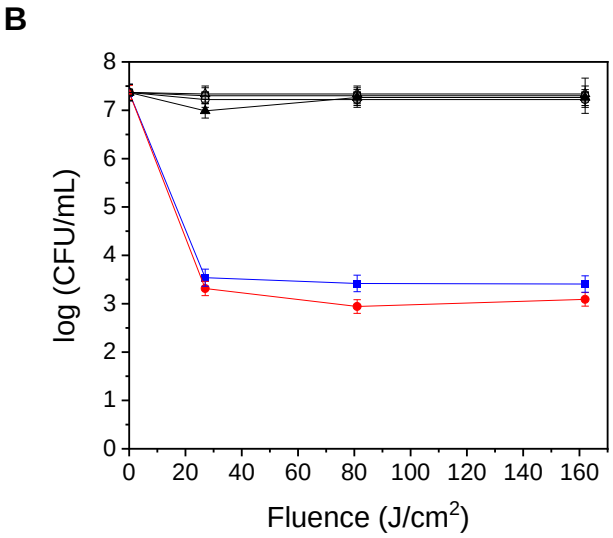


**Figure 6.** Survival curves of (A) MRSA (~$10^8$ CFU/mL) and (B) *E. coli* (~$10^8$ CFU/mL) incubated with BOPHY + 100 mM KI and irradiated for different periods (5, 15 and 30 min) with visible light (350-800 nm, 90 mW/cm$^2$): **BP** (black up-pointing triangle), **BP-Br** (blue square), and **BP-I** (red circle). Controls: bacterial cells incubated with 100 mM KI and **BP** (up-pointing triangle), **BP-Br** (square), and **BP-I** (circle) and non-irradiated. The PS concentrations were 1 μM for MRSA and 5 μM for *E. coli*.

### *Formation of iodine*

As demonstrated in PDI experiments, the use of KI is an economical approach to enhance the effectiveness of antimicrobial treatments. Though the precise mechanism of this potentiation agent remains unclear, it is established that ROS react with this nontoxic salt to form RIS, such as iodine ($I_2$) and iodine radical ($I^{\bullet}$).[22,48,49] Thus, with the purpose of demonstrating the formation of $I_2$, resulting from the ROS-induced reaction with KI, solutions of BOPHYs in DMF/$H_2O$ (95:5) and containing KI (10 mM) were irradiated under the same conditions of PDI , and absorption spectra were subsequently acquired (**Figure 7**). A Lugol solution (triiodide anion, $I_3^-$) served as a positive control, whereas solutions bubbled with argon, kept in the dark, and without PS were used as negative controls (Figure S12). As depicted in **Figure 7**, solutions containing BOPHYs and exposed to visible light presented the formation of a new absorption band centered at λ = 362 nm. Upon comparing with the absorption spectrum of Lugol, this electronic transition can be ascribed to the generation of the triiodide anion (formed by the iodine and iodide). Further, it is worth mentioning that the formation

10.1002/cptc.202400077

of $I_3^-$ did not occur in Ar-saturated solutions, BOPHY-free solutions, and solutions kept in the dark. Based on these measurements, it can be concluded that the RIS are produced as a result of the reaction between KI and the $^1O_2$ which is photosensitized by BOPHYs. Finally, in **Figure 7**, it is evident that after irradiating in aerobiosis for 5 minutes, the formation of $I_3^-$ is significantly higher for the diiodinated compound, followed by **BP-Br**.

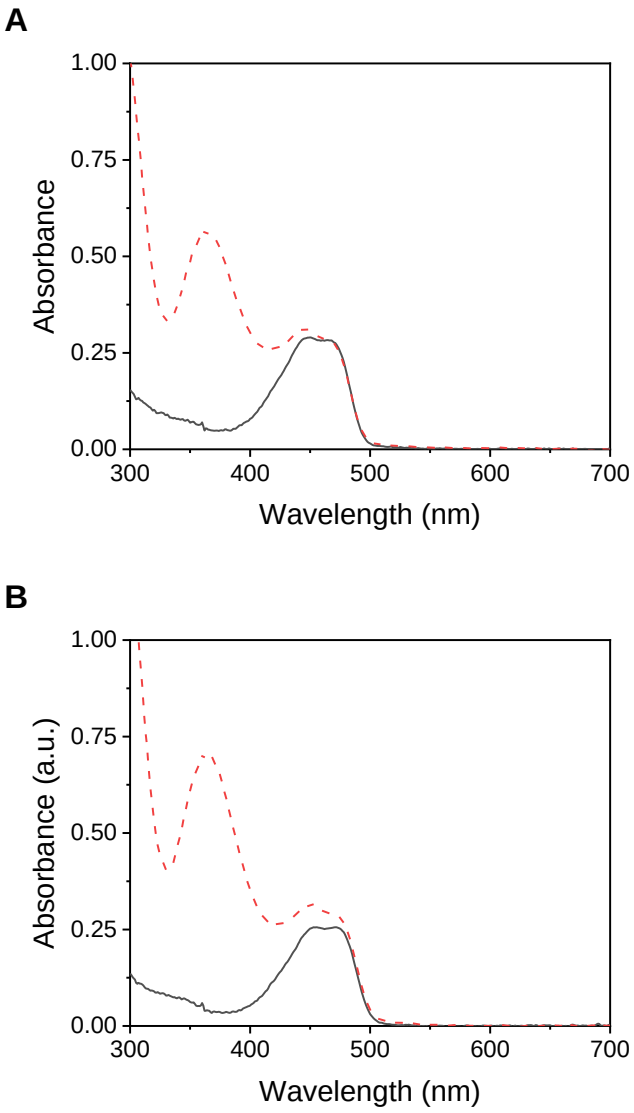


**Figure 7**. Absorption spectra of solutions containing KI (10 mM), and (A) **BP-Br** and (B) **BP-I** in DMF/$H_2O$ (5%) after 5 min of irradiation (red lines). Black lines, absorption spectra of BOPHYs. Samples were irradiated with white light (350-800 nm, 90 mW/cm$^2$). [PS] = 5 µM.

10.1002/cptc.202400077

The production of $I_3^-$ increases the effectiveness of photokilling in bacteria, but it is not the unique reactive species that can be responsible for the photoinactivation.[57] In an aqueous environment, iodide can react with $^1O_2$ to form $H_2O_2$, a ROS that improves the antimicrobial action of the PDI treatments.[57,58] In addition, this ROS is able to form $I_3^-$ by reaction with the excess of iodide.[59,60] To the best of our knowledge, to date, there is no existing report on the combination of BOPHY and KI to enhance photodynamic treatments. Therefore, our study opens up new possibilities for utilizing and potentiating BOPHY-based phototherapeutic agents with KI.

## Conclusions

We developed a practical and straightforward synthetic pathway towards the synthesis of three BOPHY derivatives, **BP** and their halogenated analogues, **BP-Br** and **BP-I**. The synthesis of each macrocycle was optimized and achieved in only four steps, with an overall reaction yield as high as ~52 %. Spectroscopic studies showed that the BOPHY derivatives have similar absorption properties regardless of the halogen atoms attached at the periphery of the macrocycle, exhibiting a slight bathochromic shift. However, the emission properties were markedly affected by the attached halogen atoms, where the emission of the diiodo derivative was almost completely quenched. In contrast, **BP** and **BP-Br** exhibited $\Phi_F$ of around 0.7 and 0.4, respectively.

Regarding the photodynamic properties, as was expected, only **BP-Br** and **BP-I** were able to produce ROS through the two photodynamic mechanisms after irradiation under aerobic conditions. Both macrocycles sensitized the production $^1O_2$ and $O_2^{\bullet-}$, being **BP-I** the most efficient PS ($\Phi_\Delta$ = 0.7). The impact of the heavy atom in **BP-I** is more pronounced, resulting in an enhancement of its photodynamic action, transforming it into a highly effective PS. Meanwhile, **BP-Br** presented a satisfactory equilibrium between ROS generation and fluorescence emission. This turns it into a promising theragnostic agent to be used in photodynamic treatments.

Binding studies by fluorescence spectroscopy demonstrated a fast binding of BOPHY derivatives MRSA after short incubation times. However, the binding of BOPHYs to *E. coli* was inefficient due to their neutral nature. The highly fluorescent macrocycle **BP** has promising properties as a fluorescent probe for cell imaging. **BP-Br** also has an adequate $\Phi_F$ for its use in this type of study as fluorescent probes.

Halogenated BOPHY derivatives exhibited efficient antimicrobial photodynamic action against MRSA, being the diiodo compound slightly more effective. However, they presented a poor performance to photoinactive *E. coli*. Thus, halogenated derivatives could be used to selectively inactivate MRSA in the presence of *E. coli*. The use of KI as a potentiating agent enabled the complete inactivation of *S. aureus* and *E. coli* using low concentrations of PS and short irradiation times. These

10.1002/cptc.202400077

conditions fulfill the primary requirements for a PS to be implemented in PDI treatments. Thus, we have conducted a PDI study using the BOPHY core as the PS for the first time.

Our outcomes underscore the advantageous impact of using KI in the PDI treatments sensitized by BOPHYs. The enhancement of the PDI action of BOPHYs, in conjunction with the use of KI, a clinically approved drug, presents a promising approach for clinical infection treatment. This work not only expands and diversifies the existing PS battery but also opens the door to the preparation of a more complex structure based on BOPHYs. The results of this investigation represent a significant milestone toward the development of novel phototherapeutic agents based on BOPHY. Furthermore, these findings will pave the way and encourage the implementation of these macrocycles in PDI.

**Acknowledgments**

Authors are grateful to Secretaría de Ciencia y Técnica, Universidad Nacional de Río Cuarto (Secyt-UNRC), Consejo Nacional de Investigaciones Científicas y Técnicas (CONICET, PIBAA 2022–2023 28720210101120CO, PIP 2021-23 PIP 11220200101208CO) and Agencia Nacional de Promoción Científica y Tecnológica (ANPCYT, PICT 02391/19) of Argentina for financial support. E.N.D., A.M.D., M.L.A., and D.A.H. are scientific members of CONICET. C.C.H., Y.B.P., E.J.G.L., and M.L. thank CONICET for doctoral fellowship.

## References

[1] K. Iskandar, J. Murugaiyan, D. Hammoudi Halat, S. E. Hage, V. Chibabhai, S. Adukkadukkam, C. Roques, L. Molinier, P. Salameh, M. Van Dongen, *Antibiotics* **2022**, *11*, 182.

[2] S. I. Ahmad, H. A. Malak, H. H. Abulreesh, *J. Glob. Antimicrob. Resist.* **2021**, *27*, 101–111.

[3] B. Plackett, *Nature* **2020,** *586*, S50–S52.

[4] F. A. Alqahtani, H. I. Almustafa, R. S. Alshehri, S. O. Alanazi, A. Y. Khalifa, *J. Pure Appl. Microbiol.* **2022**, *16*, 2201–2224.

[5] A. M. Durantini, D. A. Heredia, J. E. Durantini, E. N. Durantini, *Eur. J. Med. Chem.* **2018**, *144*, 651–661.

[6] M. S. Baptista, J. Cadet, A. Greer, A. H. Thomas, *Photochem. Photobiol.* **2023**, *99*, 313–334.

[7] M. S. Baptista, J. Cadet, A. Greer, A. H. Thomas, *Photochem. Photobiol.* **2021**, *97*, 1456–1483.

[8] M. R. Hamblin, H. Abrahamse, *Drug. Dev. Res.* **2019**, *80*, 48–67.

[9] S. Marasini, L. G. Leanse, T. Dai, *Adv. Drug Deliv. Rev.* **2021**, *175*, 113822.

[10] D. A. Heredia, A. M. Durantini, J. E. Durantini, E. N. Durantini, *J. Photochem. Photobiol. C* **2022**, *51*, 100471.

[11] L. Sobotta, P. Skupin-Mrugalska, J. Piskorz, J. Mielcarek, *Dyes Pigm.* **2019**, *163*, 337–355.

[12] L. Sobotta, P. Skupin-Mrugalska, J. Piskorz, J, Mielcarek, *Eur. J. Med. Chem.* **2019**, *175*, 72-106.

[13] E. J. Gonzalez Lopez, A. M. Sarotti, S. R. Martínez, L. P. Macor, J. E. Durantini, M. Renfige, M. A. Gervaldo, L. A. Otero, A. M. Durantini, E. N. Durantini, D. A. Heredia, *Chem. Eur. J.* **2022**, *28*, e202103884.

[14] I. S. Tamgho, A. Hasheminasab, J. T. Engle, V. N. Nemykin, C. J. Ziegler, *J. Am. Chem. Soc.* **2014**, *136*, 5623–5626.

[15] S. Boodts, E. Fron, J. Hofkens, W. Dehaen, *Coord. Chem. Rev.* **2018**, *371*, 1–10.

[16] M. Ponce-Vargas, C. Azarias, D. Jacquemin, B. Le Guennic, *J. Phys. Chem. B* **2017**, *121*, 10850–10858.

[17] Y. Li, H. Zhou, S. Yin, H. Jiang, N. Niu, H. Huang, S. A. Shahzad, C. Yu, *Sens. Actuators B* **2016**, *235*, 33–38.

[18] C. Zhang, J. Zhao, *J. Mater. Chem. C* **2016**, *4*, 1623–1632.

[19] T.-F. Cui, J. Zhang, X.-D. Jiang, Y.-J. Su, C.-L. Sun, J.-L. Zhao, *Chin. Chem. Lett.* **2016**, *27*, 190–194.

[20] L. Wu, K. Burgess, *Chem. Commun.* **2008**, *40*, 4933–4935.

[21] E. J. Gonzalez Lopez, S. R. Martínez, V. Aiassa, S. C. Santamarina, R. E. Domínguez, E. N. Durantini, D. A. Heredia, *Pharmaceutics* **2023**, *15*, 392.

[22] E. J. Gonzalez Lopez, S. C. Santamarina, M. G. Alvarez, D. A. Heredia, E. N. Durantini, *J. Photochem. Photobiol. A* **2023**, *435*, 114288.

[23] R. Schmidt, E. Afshari, *J. Phys. Chem.* **1990**, *94*, 4377–4378.

[24] Y. B. Palacios, S. C. Santamarina, J. E. Durantini, E. N. Durantini, A. M. Durantini, *J. Photochem. Photobiol. B* **2020**, *212*, 112049.

[25] X. Li, G. Ji, Y.-A. Son, *Dyes Pigm.* **2016**, *124*, 232–240.

[26] L. Wang, J-W. Wang, A-J. Cui, X-X. Cai, Y. Wan, Q. Chen, M-Y. He, W. Zhang, *RSC Adv.* **2013**, *3*, 9219–9222.

[27] S. R. Martínez, Y. B. Palacios, D. A. Heredia, M. L. Agazzi, A. M. Durantini, *ACS Infect. Dis.* **2019**, *5*, 1624–1633.

[28] Q. Huaulmé, A. Mirloup, P. Retailleau, R. Ziessel, *Org. Lett.* **2015**, *17*, 2246–2249.

[29] R. Sola-Llano, J. Jiménez, E. Avellanal-Zaballa, M. Johnson, T. A. Cabreros, F. Moreno, B. L. Maroto, G. Muller, J. Bañuelos, L. Cerdán, I. García-Moreno, S. de la Moya, *Dyes Pigm.* **2019**, *170*, 107662.

[30] X. Lv, T. Li, Q. Wu, C. Yu, L. Jiao, E. Hao, *J. Org. Chem.* **2018**, *83*, 1134–1145.

[31] A. N. Bismillah, I. Aprahamian, *Chem. Soc. Rev.* **2021**, *50*, 5631–5649.

[32] M. P. Cormick, M. G. Alvarez, M. Rovera, E. N. Durantini, *Eur. J. Med. Chem.* **2009**, *44*, 1592–1599.

[33] H. Liu, G. Jiang, G. Ke, T.-B. Ren, L. Yuan, *ChemPhotoChem* **2024**, e202300277.

[34] M. S. Baptista, J. Cadet, P. Di Mascio, A. A. Ghogare, A. Greer, M. R. Hamblin, C. Lorente, S. C. Nunez, M. S. Ribeiro, A. H. Thomas, M. Vignoni, T. M. Yoshimura, *Photochem. Photobiol.* **2017**, *93*, 912–919.

[35] F. Cieplik, D. Deng, W. Crielaard, W. Buchalla, E. Hellwig, A. Al-Ahmad, T. Maisch, *Crit. Rev. Microbiol.* **2018**, *44*, 571–589.

[36] C. Yu, L. Jiao, P. Zhang, Z. Feng, C. Cheng, Y. Wei, X. Mu, E. Hao, *Org. Lett.* **2014**, *16*, 3048–3051.

[37] G. J. Maghzal, K.-H. Krause, R. Stocker, V. Jaquet, *Free Radic. Biol. Med.* **2012**, *53*, 1903–1918.

[38] K. Krumova, G. Cosa, Chapter 1: Overview of Reactive Oxygen Species, in *Singlet Oxygen: Applications in Biosciences and Nanosciences*; Royal Society of Chemistry: Piccadilly, London, **2016**; Volume 1, pp. 1-21. ISBN 978-1-78262-220-8.

[39] N. Shankar, P.-M. Soe, C. C. Tam, *Int. J. Infect. Dis.* **2020**, *92*, 2020, 105–113.

[40] S. J. Dunn, C. Connor, A. McNally, *Curr. Opin. Microbiol.* **2019**, *51*, 51–56.

[41] E. Alves, M. A. Faustino, M. G. Neves, A. Cunha, J. Tome, A. Almeida, *Future Med. Chem.* **2014**, *6*, 141–164.

[42] M. L. Agazzi , M. B. Ballatore, E. Reynoso, E. D. Quiroga, E. N. Durantini, *Eur. J. Med. Chem.* **2017**, *126*, 110–121.

[43] D. O. Frimannsson, M. Grossi, J. Murtagh, F. Paradisi, D. F. O'Shea, *J. Med. Chem.* **2010**, *53*, 7337–7343.

[44] D. R. Rice, H. Gana, B. D. Smith, *Photochem. Photobiol. Sci.* **2015**, *14*, 1271–1281.

[45] N. Malanovic, K. Lohner, *Biochim. Biophys. Acta* **2016**, *1858*, 936–946.

[46] J. Cama, A. M. Henney, M. Winterhalter, *J. Mol. Biol.* **2019**, *431*, 3531–3546.

[47] B. Hernandez Alvarez, J. Bassler, A. N. Lupas, *Intern. J. Med. Microbiol.* **2019**, *309*, 351–358.

[48] M. R. Hamblin, *Expert Rev. Anti-Infect. Ther.* **2017**, *15*, 1059–1069.

[49] M. R. Hamblin, H. Abrahamse, *Molecules* **2018**, *23*, 3190.

[50] R. O. Costa, P. M. de Macedo, A. Carvalhal, A. R. Bernardes-Engemann, *An. Bras. Dermatol.* **2013**, *88*, 396–402.

[51] L. Huang, A. El-Hussein, W. Xuan, M. R. Hamblin, *J. Photochem. Photobiol. B* **2018**, *178*, 277–286.

[52] E. Baigorria, J. E. Durantini, S. R. Martínez, M. E. Milanesio, Y. B. Palacios, A. M. Durantini. *ACS Appl. Bio Mater.* **2021**, *4*, 8559–8570.

[53] E. Reynoso, E. D. Quiroga, M. L. Agazzi, M. B. Ballatore, S. G. Bertolotti, E. N. Durantini. *Photochem. Photobiol. Sci.* **2017**, *16*, 1524–1536.

[54] M. L. Agazzi, J. E. Durantini, E. D. Quiroga, M. G. Alvarez, E. N. Durantini, *Photochem. Photobiol. Sci.* **2021**, *20*, 327–341.

[55] A. Sułek, B. Pucelik, M. Kobielusz, A. Barzowska, J. M. Dąbrowski, *Int. J. Mol. Sci.* **2020**, *21*, 8716.

[56] J. M. D. Calmeiro, S. R. D. Gamelas, A. T. P. C. Gomes, M. A. F. Faustino, M. G. P. M. S. Neves, A. Almeida, J. P. C. Tomé, L. M. O. Lourenço, *Dyes Pigm.* **2020**, *181*, 108476.

[57] L. Huang, G. Szewczyk, T. Sarna, M. R. Hamblin, *ACS Infect Dis.* **2017**, *3*, 320–328.

[58] D. Vecchio, A. Gupta, L. Huang, G. Landi, P. Avci, A. Rodas, M. R. Hamblin, *Antimicrob. Agents Chemother.* **2015**, *59*, 5203–5212.

[59] C. Vieira, A. T. P. C. Gomes, M. Q. Mesquita, N. M. M. Moura, M. G. P. M. S. Neves, M. A. F. Faustino, A. Almeida, *Front. microbiol.* **2018**, *9*, 2665.

[60] C. Vieira, A. Santos, M. Q. Mesquita, A. T. P. C. Gomes, M. G. P. M. S. Neves, M. A. F. Faustino, A. Almeida, *J. Porphyrins Phthalocyanines* **2019**, *23*, 534–545.